

# PVP and G1.5 PAMAM dendrimer co-mediated synthesis of silver nanoparticles

Guoping Li, Yunjun Luo\*, Huimin Tan

*Department of Chemical Engineering, Polymer Division, School of Materials Science and Engineering, Beijing Institute of Technology, Number 5, Zhongguancun South St, Haidian District, Beijing 100081, PR China*

Received 7 October 2004; received in revised form 10 December 2004; accepted 15 December 2004

## Abstract

PVP and G1.5 PAMAM dendrimer co-mediated silver nanoparticles of smaller than 5 nm in diameter were prepared using H<sub>2</sub> as reducing agent. With the TEM micrograph, it was found that the molar ratios of PVP and G1.5 PAMAM dendrimer have significant effect in the morphology and size distribution of silver nanoparticles. The reaction rate (fitting a first-order equation) was strongly influenced by the molar ratios of PVP and G1.5 PAMAM dendrimer and the reaction temperature. From the UV–Vis spectra of an aqueous solution of silver nanoparticles, they could be stored for at least 2 months without coagulation at room temperature.

© 2005 Elsevier Inc. All rights reserved.

**Keywords:** PVP; PAMAM dendrimer; Silver nanoparticle; Co-mediated synthesis

## 1. Introduction

Silver nanoparticles have attracted considerable interest because of their potential applications in areas such as nanoelectronics, optical filter, electromagnetic interference shielding and surface-enhanced Raman scattering [1]. During the past few decades, many methods including both physical and chemical methods [2] have been reported in the literature for the synthesis of silver nanoparticles stabilized by polymer. For chemical methods, the choice of the reductant is of course the major factor. The common reductants can be  $\gamma$ -radiation [3], hydrazine [4], sodium boron hydride [5], etc. It is obvious that the reducing ability of reductants will determine the formation kinetics of the metal nanoparticles. At the same time, the choice of a suitable protecting agent during the course of the reduction of relevant metal salts is also important, which is necessary in controlling the growth of metal nanoparticles through

agglomeration. It has been known that silver nanoparticles can be prepared by using polyvinyl-pyrrolidone (PVP) as a protecting agent [6]. It suggested that PVP promotes the nucleation of metallic silver because silver ions are easily reduced by the lone pair electrons of PVP. Meanwhile the particles prepared by this method usually irregular in shape and the size would be larger than 100 nm. Jiang et al. reported that dendritic silver nanoparticles were prepared by ultraviolet irradiation photoreduction technique, or by sonoelectrochemical methods [7], or under microwave irradiation [8] in the presence of PVP.

Recently, dendrimer templating synthesis of metallic nanoparticles has been developed because of their unique structures, properties and their abilities to complex with a great variety of ions or compounds [9–11]. Due to the atomic/molecular level dispersion of the inorganic and organic matter, the complexes display unique physical and chemical properties of both the nanosized host and nanodispersed guest. These dendrimer nanocomposites are really composites with no covalent interaction between their components, the

\*Corresponding author. Fax: +86 10 6894 5206.

E-mail address: [yjluo@bit.edu.cn](mailto:yjluo@bit.edu.cn) (Y. Luo).

interactions between guest atoms and their microenvironment (metal–metal and metal–solvent) are substituted with the metal–dendrimer, dendrimer–solvent interactions. For this reason, the solutions of metal nanoparticles prepared using dendrimer as template may be stable for very long time in appropriately selected solvent systems. This feature is especially important in the nanoscopic region. Previous works mainly focused on the application of high-generation dendrimers. Up to now, only few reported that simple low-generation dendrimers was used to control the nanostructures of inorganic substances [12]. Low-generation dendrimers tend to exist in relative open forms, which provide reactive sites at the periphery of dendrimer, so in theory the preparation of metal nanoparticles formed inside the low-generation dendrimers is more difficult than of the high-generation dendrimers. But the low-generation dendrimers has own advantages. On the one hand, low-generation dendrimers is easier to be synthesized than high-generation dendrimers. On the other hand, the structure and chemical properties of low-generation dendrimers are very different from the liner polymers with random-coil structure [13]. It is well known that PVP is one of random-coil polymers, so it might be expected that the interesting phenomenon may be appeared using low-generation dendrimers and PVP as co-template to prepare metal nanoparticles.

In this work, PVP and low-generation dendrimers was used firstly as co-template to prepare Ag nanoparticles by  $H_2$ , called as “green reductive”, as reducing agent. UV–Vis absorption, transmission electron microscopy (TEM) and electron diffraction (ED) were employed to characterize the nanoscale structures of the resulting Ag nanoparticles. It was found that the resulted nanoparticles were dispersed, uniform and stable for months.

## 2. Experiment

### 2.1. Measurements

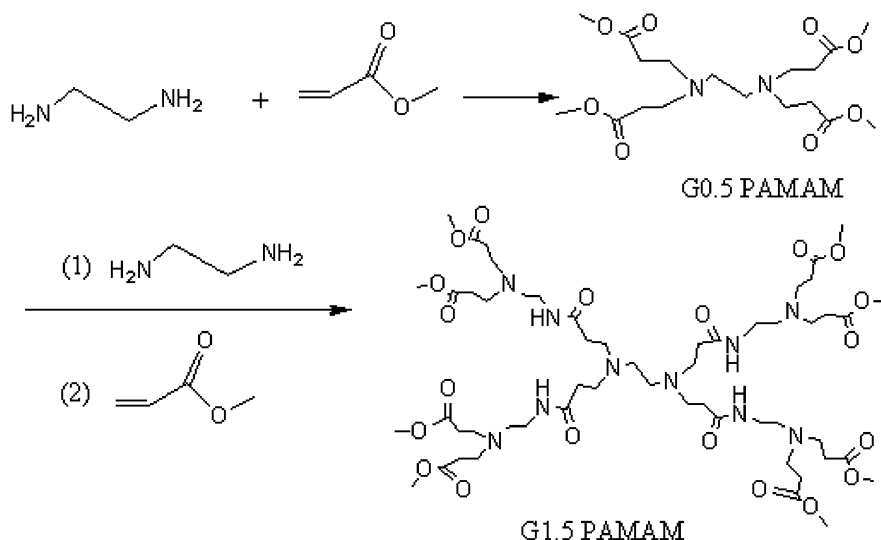
UV–Vis absorption spectra were recorded with a Unico UV-2201 UV–Vis spectrophotometer. TEM and selected area electron diffraction images of Ag nanoparticles were taken with a Hitachi modes H700A-2 apparatus. Samples for TEM and ED were prepared by dropping of colloidal dispersion of Ag onto a carbon-covered 200-mesh copper grid followed by naturally evaporating the solvent. The mean particle diameter and standard derivation were calculated by counting 100 particles from the enlarged photographs.

### 2.2. Materials

High purity silver nitrate ( $AgNO_3$ ),  $H_2$  and sodium borohydride ( $NaBH_4$ ), were purchased from Beijing Chemical Company of China, and were used without further purification. PVP (K30, polymerization degree 360) was purchased from the United States. G1.5 PAMAM dendrimers (G1.5) were synthesized by ourselves, as shown in Scheme 1.

### 2.3. Synthesis of Ag nanoparticles

PVP, G1.5 PAMAM and  $AgNO_3$  were dissolved in deionized water to form an aqueous solution of PVP (0.01 M), G1.5 PAMAM (0.01 M) and  $AgNO_3$  (0.1 M), respectively. Then, the aqueous solution of PVP (0.01 M), G1.5 PAMAM (0.01 M) and  $AgNO_3$  (0.1 M) were mixed at a volume ratios of 1:0:1(A), 1:1:1 (B), 0:1:1 (C), respectively. The colorless solution of  $AgNO_3$  turned to yellow upon mixing with the mixed solution of



Scheme 1. Synthesis of G1.5 PAMAM dendrimer.

PVP and G1.5 PAMAM, which indicated the formation of a salt between protonized nitrogen of PVP or G1.5 PAMAM and Ag anions [6,14]. The above mixed solutions were added into a two-neck round bottom flask, which was full of  $H_2$ , by syringe. The reaction time began to be recorded, as soon as the reaction solution was stirred. The reaction was stopped for every scheming time for characterization. During the course of the reduction reaction,  $H_2$  flowed into the reaction vessel in order to keep the pressure constant of the reaction vessel and the reaction temperature was kept at room temperature. It was found that the color of the solution changed from yellow to deep red indicated the reduction of Ag anions coordinated to nitrogen of PVP or G1.5 PAMAM into zerovalent Ag.

### 3. Results and discussion

#### 3.1. Formation of silver nanoparticles

The stabilization of Ag nanoparticles in aqueous solution by PVP and G1.5 PAMAM dendrimer is possible over a wide range conditions. To control the size and the morphology of the particles, one needs to optimize the molar ratios of the added  $Ag^+$  ions and PVP and dendrimer, and the reduction rate. In the first step, the PVP/G1.5 PAMAM dendrimer/Ag ions has to be adjusted so that no precipitation occurs. Therefore, there solution tailored A, B and C as described above in which no precipitation could be found. It was found that PVP or G1.5 PAMAM dendrimer was an effective template only when sufficiently slow reduction rates were used. So in this work, the green reductive,  $H_2$ , the reduction rate of which is slow, was employed to reduce  $Ag^+$  ions to Ag atoms.

Fig. 1 shows UV–Vis spectra of the stable aqueous solution of Ag nanoparticles with different molar ratios of PVP to G1.5 PAMAM dendrimer to Ag. The obtained solution showed absorption bands at 459(A), 407(B), and 417 nm(C), respectively, which are assigned to the surface plasmon resonance of the obtained Ag nanoparticles, when the molar ratios of PVP/G1.5 PAMAM dendrimer/Ag were 2:0:1, 1:1:1 and 0:2:1. According to Mie's theory [15], the position and shape of the adsorption peaks, which are attributed to the surface plasmon resonance, are affected by the nature of the metal, the size and shape of the nanoparticles, and the status of aggregation of the particles [16]. The surface plasmon peak shifts to a longer wavelength and is broadened when well-isolated particles form the other shape particles (for example, dendritic silver particles). One could see that the shift of maximum adsorption wavelength between under the condition A (459 nm) and under the condition B (407 nm). The red shift of the maximum adsorption wavelength could be explained as

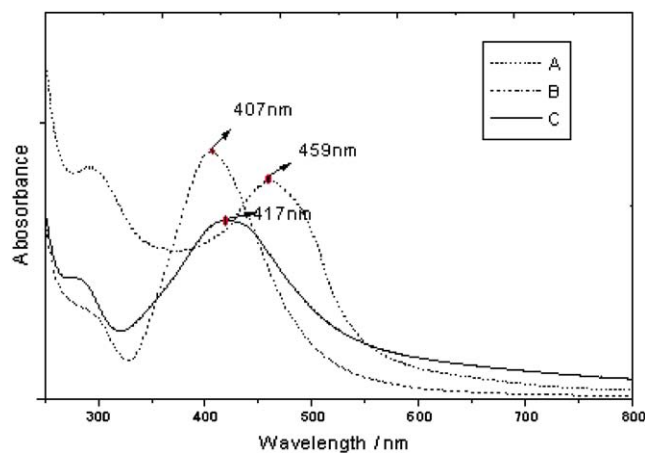
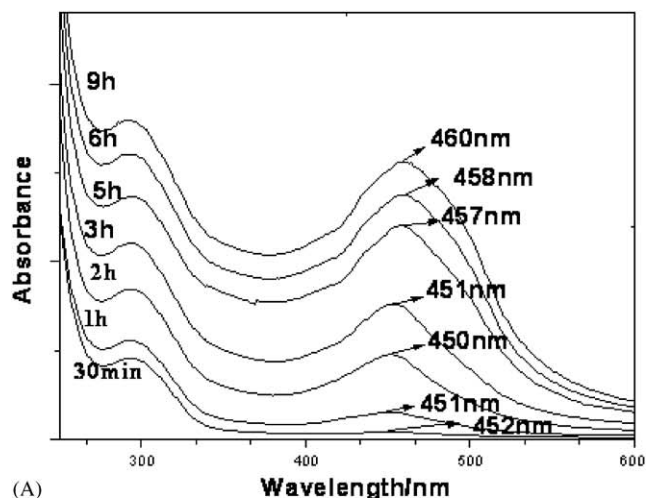


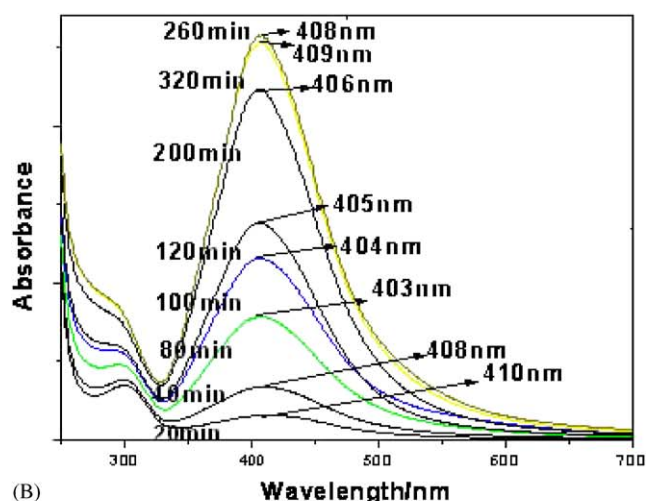
Fig. 1. UV–Vis spectra of Ag nanoparticles under reaction conditions A, B, and C, respectively.

formation of the different shape silver nanoparticles. And comparing with the absorption peak (C), the symmetry of the absorption peak (B) was relatively best and its full-width at half-maximum (FWHM) was relatively smallest, which indicated that Ag nanoparticles prepared under the condition B were much most uniform in size. The results were in good agreement with the later TEM analysis.

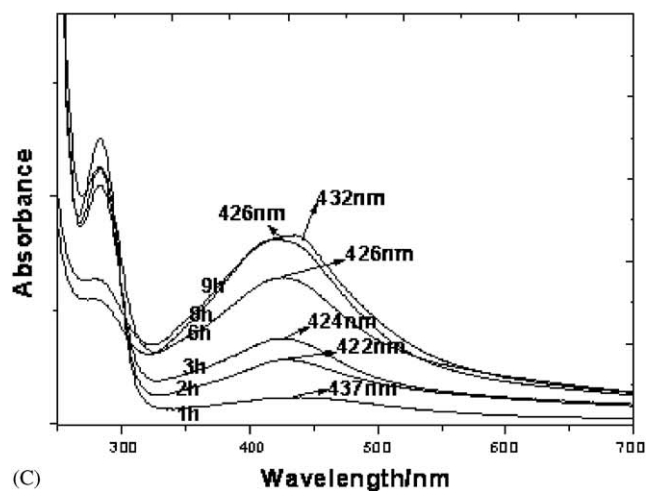
The formation process of Ag nanoparticles was monitored by UV–Vis absorption spectrum. Fig. 2 shows the peak shift and the shape of absorption spectra during the whole reaction. The time was set when the reaction vessel was aerated with the reduction agent  $H_2$  as the starting time. With the increase of time, a clear peak appeared and its position changed, e.g., 452 nm at 30 min, 451 nm at 1 h, 450 nm at 2 h, 451 nm at 3 h, 457 nm at 6 h, 458 nm at 8 h and 460 nm at 9 h under the reaction condition A; 410 nm at 20 min, 408 nm at 40 min, 403 nm at 80 min, 404 nm at 100 min, 406 nm at 120 min, 408 nm at 200 min, 408 nm at 260 min, and 409 nm at 320 min under the reaction condition B; 437 nm at 1 h, 422 nm at 2 h, 424 nm at 3 h, 426 nm at 6 h, 426 nm at 8 h, and 432 nm at 9 h under the reaction condition C. From this series of peak position changes, it was concluded that the peak kept the blue shift at the first stage of reaction, being due to increasing electron cloud around the obtained Ag particles from N atoms of PVP or dendrimer. However then the peak position turned to the red shift, which is the result of the increasing size of Ag particles. At the latest stage the peak position kept constant, which was indicated that the silver nanoparticles stopped their growth in size. Comparing with the reaction conditions A and C, the reduction rate was relatively faster under the reaction condition B. This result gave the evidence that there is a synergistic effect between PVP and dendrimer resulting in the electrons easily transferring from PVP or dendrimer to Ag ions.



(A)



(B)



(C)

Fig. 2. UV-Vis spectrum of Ag nanoparticles at different reaction time during reaction process under reaction conditions A, B, and C (Note: the vertical order did not show the exact absorbance value and left number was reaction time and right number was value of  $\lambda_{\max}$ ).

The absorption spectra of the obtained silver particles system were measured at different shelf time so as to investigate its stability. From Fig. 3, it was observed that

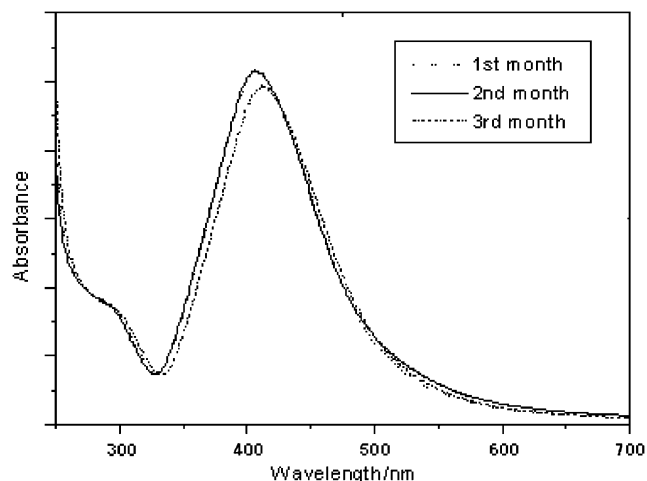


Fig. 3. UV-Vis spectra of Ag nanoparticles obtained under the reaction condition B and stored in 3 months.

the absorption spectra of silver particles system had no obvious difference in shape, position and symmetry in the first 2 month. After the third month, the peak position of absorption spectrum had a slight red shift, which implied that the Ag nanoparticles started to aggregate. So the silver nanoparticles prepared under the reaction condition B could remain stable at least 2 months.

### 3.2. Kinetics of Ag nanoparticles formation

The process of Ag nanoparticles formation was traced by UV-Vis spectra under the different molar ratios of reactants or reaction temperatures. In Fig. 4(a), the dependency on the molar ratios of PVP and G1.5 PAMAM dendrimer (at constant temperature 20 °C and  $[\text{AgNO}_3]$  0.1 M) was showed, while (b) figure indicated the influence of reaction temperature (under the reaction condition B). It can be observed that the formation rate was relatively faster under high temperature and decreased with time. From Fig. 4, it came out that the molar ratios of PVP and G1.5 PAMAM dendrimer determined the final maximum absorbance value, i.e., the final size and number of prepared silver nanocrystals, and the reduction rate. At the same time the temperature settled the reaction rate. That the three plots started from almost the same point revealed that the reduction was greatly slow at the very beginning of the reaction and the reaction rate was relatively faster when PVP and G1.5 PAMAM dendrimer was co-protecting agent, which agreed with that of Fig. 2.

The absorbance time dependence in Fig. 4 could be fit by first-order rate equation with high reliability:

$$A(t) = A_1(1 - e^{-kt}),$$

where  $A(t)$  is the absorbance at the time  $t$ ,  $A_1$  the absorbance at a very long time,  $t$  the different time, and

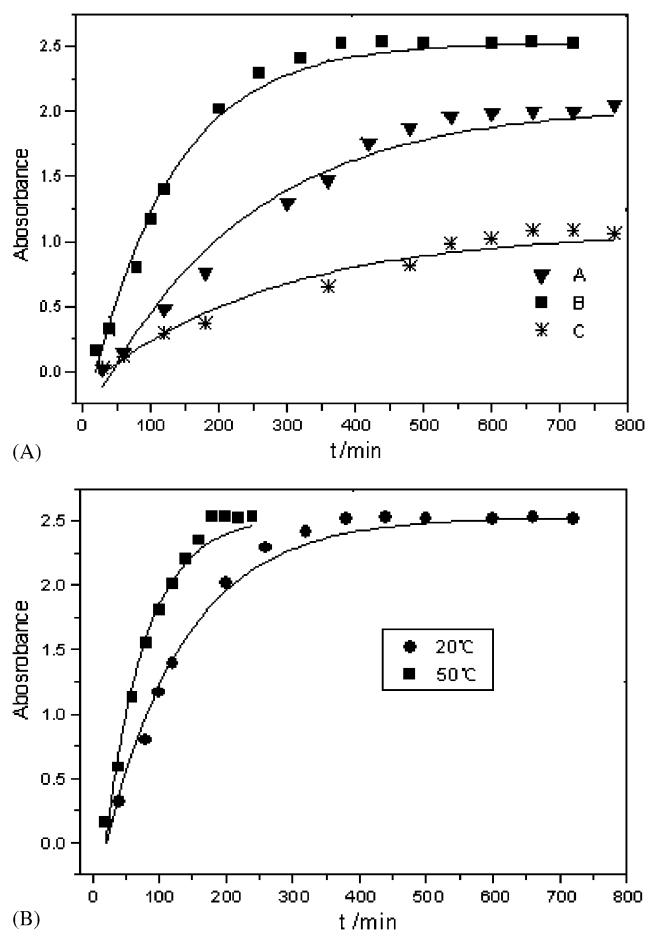


Fig. 4. Evolution of Ag nanoparticles' absorbance, left: at 20 °C at different reaction conditions A, B, C, respectively,  $[\text{AgNO}_3]$  0.1 M; right: under the reaction condition B.

$k$  the first-order rate constant. The fit result was in Table 1.

### 3.3. Transmission electron micrographs and electron diffraction

An obvious different morphology could be observed from the TEM micrograph of various molar ratios of PVP and half-generation PAMAM dendrimer (Fig. 5). When the molar ratios of PVP and G1.5 PAMAM dendrimer and  $\text{AgNO}_3$  was 2:0:1, the morphology of the product was dendritic (Fig. 5A), while the discrete nanoparticles (Fig. 5B and C) would be obtained as the molar ratios of PVP and G1.5 PAMAM dendrimer and  $\text{AgNO}_3$  was 1:1:1 and 0:2:1. From Fig. 5C where the protecting agent was G1.5 PAMAM dendrimer, the mean diameter of silver nanoparticles was determined to be 7.85 nm, and the standard deviation was 1.60 nm. The diameter of G1.5 PAMAM dendrimer was estimated on the basis of molecular modeling calculation to be approximately 2.8 nm, whose radius is smaller than the diameter of silver nanoparticles. On the basis of these

Table 1

First-order constant results from fits by Eq. (1) to the time evolution of Ag nanoparticles' absorbance

Molar ratios of PVP, G1.5 PAMAM and $\text{AgNO}_3$	$T$ (°C)	$A_1$	$k$ ( $\text{min}^{-1}$ )
2:0:1 (A)	20	2.05	0.0044
1:1:1 (B)	20	2.53	0.0083
0:2:1 (C)	20	1.08	0.0037
1:1:1 (B)	50	2.53	0.016

facts, most of silver nanoparticles are surrounded by G1.5 PAMAM dendrimer. While in Fig. 5B where PVP and G1.5 PAMAM dendrimer co-existed, the morphology of nanoparticles was almost spherical and the mean diameter was 4.79 nm ( $\sigma = 0.97$ ), i.e., to say, the size distribution was relatively narrow. Consequently, the FWHM of absorption spectra was smallest (see Fig. 1). We may conclude accordingly that PVP and G1.5 PAMAM dendrimer co-mediate showed best template performance.

The selected area ED of Ag nanoparticles prepared under the condition B was shown in Fig. 5B. The characteristic rings in polycrystalline diffraction pattern could be indexed to the {111}, {200}, {220} and {300} allowed reflecting planes expected from face center cubic Ag. This fact presented an unambiguous proof for formation of Ag (0) particles under the experimental condition used.

### 3.4. X-ray diffraction patterns

Fig. 6 showed the power XRD patterns of as prepared PVP–G1.5 PAMAM co-stabilized Ag nanoparticles. The reflection peaks at  $2\theta$  of 38.5°, 43.5° and 64.5° correspond to the 111, 200, 220 and 311 crystal planes, respectively. They are well consistent with JCPDS files (No. 41-1402) and indicate that the gained Ag nanoparticles are of face-centered cubic. The results were in good agreement with the ED analysis.

## 4. Conclusion

Well-dispersed silver nanoparticles with smaller than 5 nm size and spherical shape has been prepared by reducing silver nitrate with  $\text{H}_2$  in the presence of PVP and G1.5 PAMAM dendrimer as a co-protective agent. The molar ratios of PVP and G1.5 PAMAM dendrimer have significant effect in the morphology and size of the obtained Ag nanoparticles. From the UV–Vis absorption spectra of Ag nanoparticles, it can be found that the reaction rate was strongly influenced by molar ratios of PVP and G1.5 PAMAM dendrimer (abiding by a first-order rate equation) and by temperature. Especially,

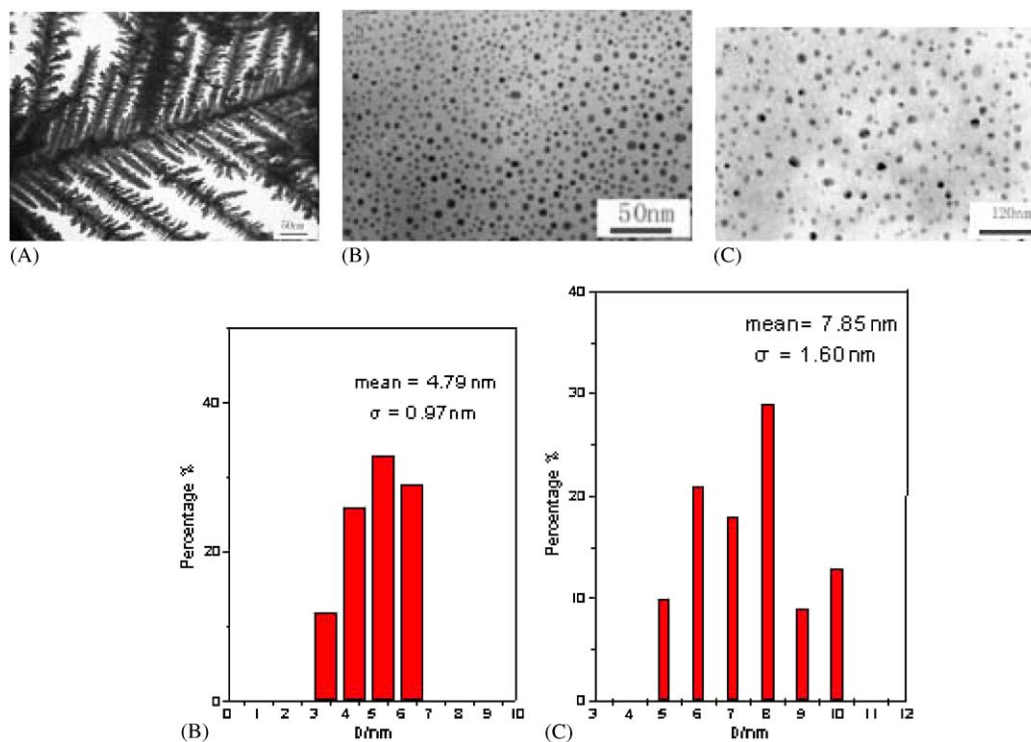


Fig. 5. The TEM micrographs of Ag nanoparticles when the molar ratios of PVP, G1.5 PAMAM dendrimer and  $\text{AgNO}_3$  was 2:0:1 (A), 1:1:1(B) and 0:1:2 (C), respectively, and the size distribution of obtained silver nanoparticles under the condition B (B) and C (C), and the electron diffraction of silver nanoparticles under condition B (B).

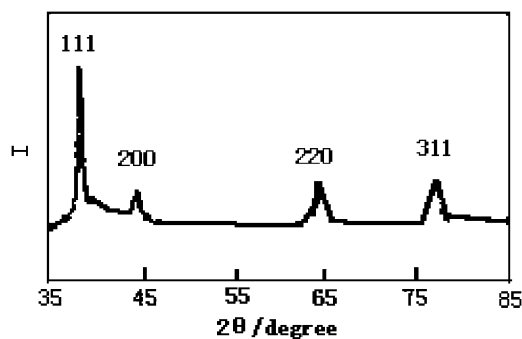


Fig. 6. XRD pattern of PVP-G1.5 PAMAM dendrimer co-mediated silver nanoparticles.

PVP-G1.5 PAMAM dendrimer/Ag formed stable colloid and could be stored for months without coagulation at room temperature.

## References

- [1] A.C. Templeton, A.W.P. Wuelfing, R.W. Murray, *Acc. Chem. Res.* 33 (2000) 27.
- [2] K.S. Chou, C.Y. Ren, *Mater. Chem. Phys.* 64 (2000) 241.
- [3] S.H. Shin, H.J. Yang, S.B. Kim, M.S. Lee, *J. Colloid Interface Sci.* 274 (2004) 89.
- [4] H. Zheng, J. Liang, J. Zeng, *Mater. Res. Bull.* 36 (2001) 398.
- [5] N. Jana, L. Gearheart, L. Murohy, *Chem. Mater.* 13 (2001) 2313.
- [6] Z. Zhang, B. Zhao, L. Hu, *J. Solid State Chem.* 121 (1996) 105.
- [7] L.P. Jiang, A.N. Wang, Y. Zhao, J.R. Zhang, J.J. Zhu, *Inorg. Chem. Comm.* 7 (2004) 506.
- [8] R. He, X.F. Qian, J. Yin, Z.K. Zhu, *Chem. Phys. Lett.* 369 (2003) 454.
- [9] X.F. Qian, J. Yin, S. Teng, S.H. Lin, Z.K. Zhu, *J. Mater. Chem.* 11 (2001) 2504.
- [10] P. Yan, H.F. Liu, K.Y. Liew, *J. Mater. Chem.* 11 (2001) 3387.
- [11] K. Esumi, A. Suzuki, A. Yamahia, K. Torigoe, *Langmuir* 16 (2000) 2604.
- [12] C. Bao, M. Jin, R. Lu, T. Zhang, Y. Zhao, *Mater. Chem. Phys.* 81 (2003) 160.
- [13] D.A. Tomalia, H. Baker, J. Dewald, M. Hall, G. Kallos, S. Martin, J. Roeck, J. Ryder, P. Smith, *Polymer* 17 (1985) 117.
- [14] G.P. Li, Y.J. Luo, H.C. Xu, Y.X. Cui, H.M. Tan, *Chinese J. Inorg. Chem.* 19 (2003) 1212.
- [15] U. Kreibitz, M. Vollmer, *Optical Properties of Metal Clusters (M): Spring Series in Materials Science*, 1995.
- [16] J. Nedderson, G. Chumanov, T.M. Cotton, *Appl. Spectrosc.* 47 (1993) 1959.